Brain, Behavior, and Immunity xxx (2016) xxx–xxx

Contents lists available at ScienceDirect

Brain, Behavior, and Immunity

journal homepage: www.elsevier.com/locate/ybrbi

Full-length Article

MHCI promotes developmental synapse elimination and aging-related synapse loss at the vertebrate neuromuscular junction

Mazell M. Tetruashvily [a,b,1], Marin A. McDonald [c,d,1], Karla K. Frietze [a], Lisa M. Boulanger [a,c,e,*]

[a] Department of Molecular Biology, Princeton University, Princeton, NJ 08544, United States
[b] Rutgers Robert Wood Johnson Medical School, Piscataway, NJ 08854, United States
[c] Department of Neurosciences, University of California, San Diego 92093, United States
[d] Medical Scientist Training Program, University of California, San Diego 92093, United States
[e] Princeton Neuroscience Institute, Princeton University, Princeton, NJ 08544, United States

ARTICLE INFO

Article history:
Received 14 September 2015
Received in revised form 12 January 2016
Accepted 12 January 2016
Available online xxxx

Keywords:
MHCI
Major histocompatibility complex class I
Neuromuscular junction
NMJ
Synapse elimination
Aging
Development
Denervation

ABSTRACT

Synapse elimination at the developing neuromuscular junction (NMJ) sculpts motor circuits, and synapse loss at the aging NMJ drives motor impairments that are a major cause of loss of independence in the elderly. Here we provide evidence that at the NMJ, both developmental synapse elimination and aging-related synapse loss are promoted by specific immune proteins, members of the major histocompatibility complex class I (MHCI). MHCI is expressed at the developing NMJ, and three different methods of reducing MHCI function all disrupt synapse elimination during the second postnatal week, leaving some muscle fibers multiply-innervated, despite otherwise outwardly normal synapse formation and maturation. Conversely, overexpressing MHCI modestly accelerates developmental synapse elimination. MHCI levels at the NMJ rise with aging, and reducing MHCI levels ameliorates muscle denervation in aged mice. These findings identify an unexpected role for MHCI in the elimination of neuromuscular synapses during development, and indicate that reducing MHCI levels can preserve youthful innervation of aging muscle.

© 2016 Elsevier Inc. All rights reserved.

1. Introduction

Synapse elimination sculpts mature patterns of connectivity throughout the vertebrate nervous system. During prenatal and early postnatal development, axons retract, refining initially diffuse projections. Consistent with a critical role in circuit maturation, defects in synapse elimination have been implicated in neurodevelopmental disorders (e.g., (Hayashi-Takagi et al., 2014; Krey et al., 2013; Noutel et al., 2011; Pfeiffer et al., 2010; Tang et al., 2014; Tsai et al., 2012)). Synapse loss also occurs with aging, when it is associated with significant motor and cognitive impairments (reviewed in (Hedden and Gabrieli, 2004; Rudolf et al., 2014)). However, the molecular drivers of developmental synapse elimination remain largely unknown. Furthermore, it is unclear if developmental synapse elimination and aging-related denervation occur through related, or distinct, molecular mechanisms.

The canonical model for studying developmental synapse elimination is the vertebrate neuromuscular junction (NMJ) (Brown et al., 1976; Thompson, 1985). Before birth, each muscle fiber receives inputs from many motor neurons (MNs) (Nguyen and Lichtman, 1996; Sanes and Lichtman, 1999; Tapia et al., 2012). MN axon branches are extensively pruned, and by the end of the second postnatal week in rodents, each muscle fiber receives input from only a single MN (Brown et al., 1976; Busetto et al., 2000; Keller-Peck et al., 2001; Personius and Balice-Gordon, 2001; Redfern, 1970).

Previous studies have significantly advanced our understanding of the factors that control the rate of synapse elimination. Several manipulations either delay (Je et al., 2013; Lee et al., 2011; Li et al., 2004; Misgeld et al., 2002; Nguyen et al., 1998; Personius et al., 2008; Rafuse et al., 2000; Roche et al., 2014; Sleigh et al., 2014; Thompson et al., 1979) or accelerate (Bogdanik et al., 2012; O'Brien et al., 1978; Personius et al., 2007; Thompson, 1983) synapse elimination at the developing NMJ. However, in most cases where synapse elimination is delayed, uniform monoinnervation is still established within the first few postnatal weeks. Thus the endogenous factors that ensure elimination of every excess MN input remain largely unknown.

* Corresponding author at: Princeton Neuroscience Institute, Princeton University, Princeton, NJ 08544, United States.
E-mail address: lboulang@princeton.edu (L.M. Boulanger).
[1] Authors contributed equally.

http://dx.doi.org/10.1016/j.bbi.2016.01.008
0889-1591/© 2016 Elsevier Inc. All rights reserved.

Please cite this article in press as: Tetruashvily, M.M., et al. MHCI promotes developmental synapse elimination and aging-related synapse loss at the vertebrate neuromuscular junction. Brain Behav. Immun. (2016), http://dx.doi.org/10.1016/j.bbi.2016.01.008

In adults, responses to peripheral motor neuron injury are regulated by specific immune proteins, members of the major histocompatibility complex, class I (MHCI). MHCI has been detected in adult motor neurons (Edstrom et al., 2004; Linda et al., 1999; Thams et al., 2009), but adult muscle cells are thought to represses MHCI genes, except after injury or in disease states (Karpati et al., 1988). Consequently, studies of the role of MHCI in the peripheral nervous system have focused almost exclusively on responses to injury. In injury models, reducing MHCI expression exacerbates loss of synapses made onto axotomized motor neuron cell bodies in the spinal cord, and impairs functional recovery (Berg et al., 2013; Oliveira et al., 2004; Thams et al., 2009). These and other studies have reinforced the view that at the NMJ, MHCI is primarily involved in responses to injury. In the central nervous system, MHCI has been implicated in pruning of developing retinal projections (Datwani et al., 2009; Huh et al., 2000; Lee et al., 2014), while elimination of developing cerebellar climbing fibers is MHCI-independent (Letellier et al., 2008; McConnell et al., 2009). Here we explored if MHCI plays a role in developmental synapse elimination or aging-related synapse loss at the vertebrate NMJ.

2. Results

2.1. Impaired synapse elimination in mice deficient for cell-surface MHCI

MHCI genes are expressed at the NMJ as synapse elimination is occurring (Tetruashvily et al., in press). If MHCI promotes synapse elimination at the developing NMJ, then reducing MHCI expression should increase the number of multiply-innervated muscle fibers. To test this prediction, we visualized innervation of postsynaptic sites in diaphragm muscle fibers from mice lacking stable cell-surface expression of most MHCI proteins ($\beta2m^{-/-}TAP^{-/-}$ mice; see Section 4). The diaphragm is a thin, planar muscle with a well-organized end plate band that is particularly amenable to imaging in whole-mount preparations. Postsynaptic nicotinic acetylcholine receptors (nAChRs) were labeled using tetramethyl rhodamine-conjugated α-bungarotoxin (α-btx), and presynaptic motor neuron axons were visualized using antibodies against the axon cytoskeletal element neurofilament and the presynaptic vesicle protein SV2. Because individual nAChR clusters may lay above one another in whole mount muscle, 3D reconstructions of confocal Z-stacks were created for all suspected multiply-innervated postsynaptic sites, and reconstructed stacks were viewed from multiple depths and angles to determine if motor neuron branches were distinct, and if they innervated a single nAChR cluster, or two clusters in different focal planes (see Section 4).

In WT mice, nearly all postsynaptic sites are contacted by a single MN axon by postnatal day 15 (P15), as expected (Kopp et al., 2000; Redfern, 1970). In contrast, significantly more postsynaptic sites remain multiply-innervated in mice lacking cell-surface MHCI (Fig. 1A–C. Multiple innervation at P15: $\beta2m^{-/-}TAP^{-/-}$, 16.4 ± 2.2%; WT, 3.5 ± 1.1%; $p = 0.0011$). Multiply-innervated postsynaptic sites detected in P15 MHCI-deficient mice all received two inputs. Although multiple innervation persists, $\beta2m^{-/-}TAP^{-/-}$ mice are of normal size and weight, and eye opening, fur growth, weaning, and reproduction all occur at appropriate ages. Development of the NMJ is also otherwise outwardly normal. Every muscle fiber contains only a single postsynaptic nAChR cluster at P15, and the area, perimeter, and intensity of nAChR labeling, and morphology of the end plate band, are all normal in $\beta2m^{-/-}TAP^{-/-}$ mice (Fig. S2). Furthermore, the distribution of nAChR labeling changes as expected from plaque-like to pretzel-like as the animals matured. Despite this maturation, multiple innervation persists in MHCI-deficient adults (Fig. 1A–C; $\beta2m^{-/-}TAP^{-/-}$, 18.6 ± 4.3%; WT, 2.3 ± 1.7%; $p = 0.0116$), and remarkably, is still present at one year of age (Fig 1D; $\beta2m^{-/-}TAP^{-/-}$, 9.5 ± 1.3%; WT, 2.5 ± 0.5%; $p = 0.0069$). Thus loss of MHCI prevents multiple innervation from fully resolving at the NMJ.

Loss of MHCI could cause multiply-innervated muscle fibers to persist because it directly or indirectly disrupts synapse elimination, or because it increases synapse formation via changes in neurogenesis, programmed cell death, or motor neuron outgrowth or branching. However, several lines of evidence suggest that changes in synapse formation do not underlie the persistent multiple innervation in MHCI-deficient animals. At birth (P0) and at P7, when MN programmed cell death and synapse formation are largely complete (Tapia et al., 2012; Xu et al., 2006; Yamamoto and Henderson, 1999), a normal proportion of postsynaptic sites are multiply-innervated in MHCI-deficient mice (Fig. 1A–C). Furthermore, at P7, each muscle fiber is contacted by the same average number of axons in WT and MHCI-deficient mice (Fig. S2E and F). Thus measures that are sensitive to changes in motor neuron and muscle fiber number and synapse formation are normal in MHCI-deficient mice. These results suggest that in the absence of MHCI, patterns of innervation are established normally, but innervation fails to decline over the second postnatal week, consistent with a disruption of developmental pruning.

However, it is still possible that loss of MHCI prevents the establishment of monoinnervation without changes in synapse elimination, e.g., by prolonging neurogenesis, programmed cell death, and/or synapse formation well past their normal developmental window. If synapse elimination is not impaired in MHCI-deficient mice, then ongoing synapse formation would be necessary to explain the stable synapse density from P7 onwards. However, we did not see evidence of ongoing axon sprouting, outgrowth, or synapse formation over the second postnatal week. Together, these results suggest that changes in synapse formation are unlikely to contribute significantly to persistent multiple innervation in MHCI-deficient animals. Instead, they are more consistent with a role for MHCI in allowing synapse elimination to reach completion.

Extensive synapse elimination occurs at the NMJ prior to the close of the first postnatal week (Tapia et al., 2012). This initial synapse elimination does not require MHCI, because at P7, the percentage of postsynaptic sites that remain multiply-innervated (Fig. 1) and the extent of MN convergence onto individual postsynaptic sites (Fig. S2E and F) are both normal in MHCI-deficient mice. Consistent with the fact that early synapse elimination happens normally, MHCI-deficient mice do not display gross motor deficits (e.g., weakness, inactivity, or tremor) (McConnell et al., 2009; Nelson et al., 2013). Over the second postnatal week, however, far fewer postsynaptic sites achieve mono-innervation in MHCI-deficient animals, a failure of circuit maturation that could disrupt the emergence of fine motor control. Remarkably, there is no further decline in multiply-innervated postsynaptic sites between P15 and adulthood (Fig. 1B and C).

2.2. Loss of MHCI impairs synapse elimination specifically during the second postnatal week

If MHCI is specifically involved in synapse elimination during the second postnatal week, then acutely disrupting MHCI function during the second postnatal week should cause multiple innervation to persist. To test this hypothesis, we inhibited MHCI function from P7-P15, using an anti-MHCI antibody (OX18) that is function-blocking in multiple assays. Incubating hepatocytes or tumor cells in OX18 is sufficient to trigger lysis by NK cells (Blom et al., 1999; Smits et al., 1994), a sensitive and specific bioassay for loss of MHCI function. OX18 recognizes MHCI in Western blots and immunohistochemistry from mouse nervous system samples (e.g., (Adelson et al., 2012; Corriveau et al., 1998; Datwani et al., 2009; Dixon-Salazar

Please cite this article in press as: Tetruashvily, M.M., et al. MHCI promotes developmental synapse elimination and aging-related synapse loss at the vertebrate neuromuscular junction. Brain Behav. Immun. (2016), http://dx.doi.org/10.1016/j.bbi.2016.01.008

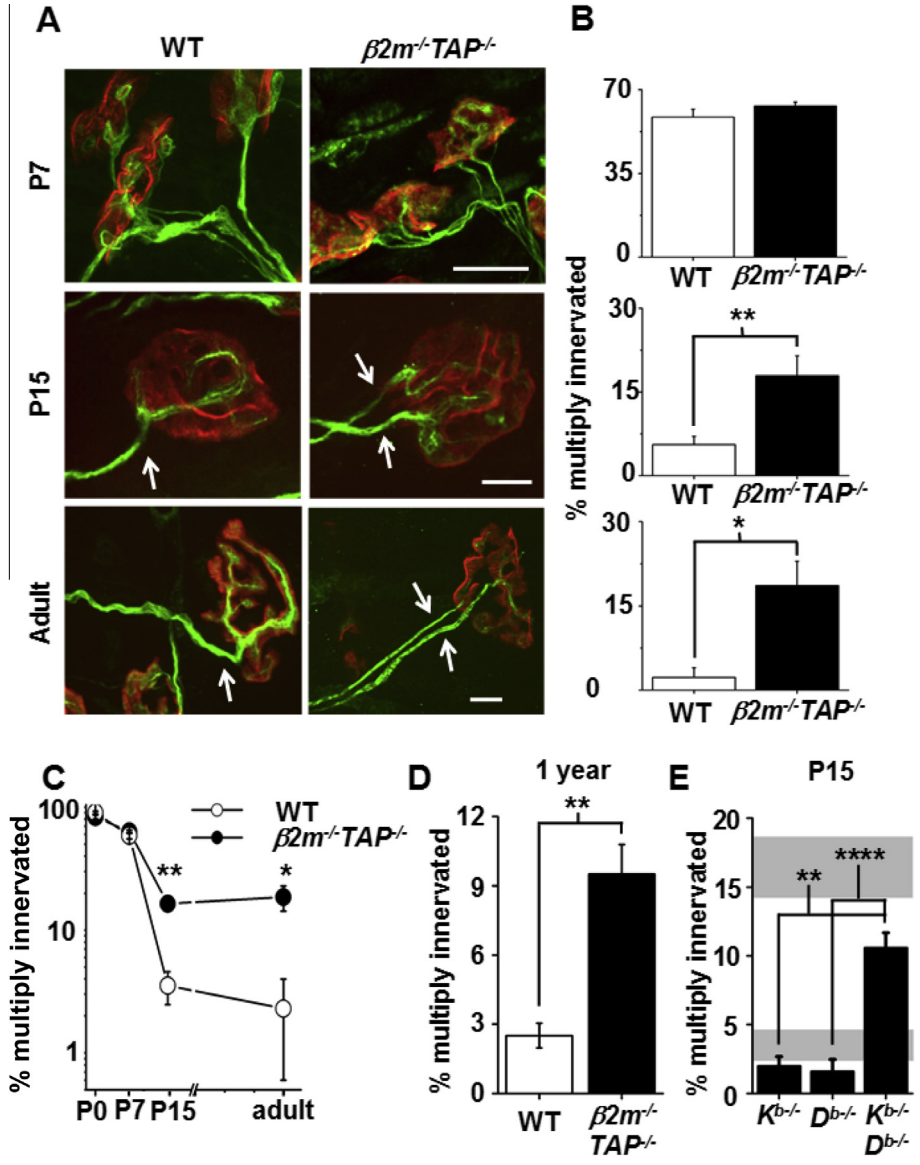


Fig. 1. Persistent multiple innervation at the MHCI-deficient NMJ. (A) Confocal images of intact muscle stained with α-btx (red) and anti-neurofilament and anti-SV2 (green). Scales, 10 μm. Arrows mark distinct MN axons in P15 and adult. (B) Multiple innervation in confocal images. Multiple innervation at P7, 63.1 ± 1.7% in $\beta2m^{-/-}TAP^{-/-}$ ($n = 6$) vs. 58.5 ± 3.3% in WT ($n = 8$), $p = 0.28$. P15, $\beta2m^{-/-}TAP^{-/-}$ $n = 9$, WT $n = 8$; adult (P29–50), $n = 4$ per genotype (values, see text). (C) Time course of synapse elimination. Multiple innervation at P0, 83.3 ± 3.1% in $\beta2m^{-/-}TAP^{-/-}$ vs. 90.2 ± 4.6% in WT, $p = 0.13$, $n = 4$ animals per genotype. (B) and (C), $^{**}p = 0.0011$; $^{*}p = 0.0116$. (D) Multiple innervation in one year old diaphragm. $\beta2m^{-/-}TAP^{-/-}$ $n = 5$, WT $n = 3$. $^{**}p = 0.0069$. (E) Multiple innervation in mice lacking classical MHCIs. $K^{b-/-}$, $n = 3$; $D^{b-/-}$, $n = 6$. Gray bars, multiple innervation (mean ± SEM) at the same age in $\beta2m^{-/-}TAP^{-/-}$ (top) or WT (bottom) diaphragm, from (B). $^{**}p = 0.002$; $^{****}p \leqslant 0.0001$.

et al., 2014; Goddard et al., 2007; Huh et al., 2000; Needleman et al., 2010)). Remarkably, injected antibodies cause a nearly threefold increase in the retention of multiple inputs relative to IgG1-injected littermate controls (Fig. 2). The quantitatively smaller effect of antibody injection compared to genetic MHCI deficiency is not surprising, for three reasons: (1) antibody penetration may not be complete, resulting in only partial block of MHCI function at the NMJ; (2) antibody is delivered transiently, and may be gradually cleared, resulting in only a temporary block of MHCI function over the week-long experiment; and (3) antibody may not completely block the function of all of the MHCI proteins whose cell-surface expression is reduced in genetically MHCI-deficient mice (see Section 4). The results of these antibody injections show that interfering with MHCI function over the second postnatal week significantly impairs establishment of monoinnervation in WT animals. Since MN cell death and synapse formation were complete before MHCI function was blocked (Tapia et al., 2012; Xu et al., 2006; Yamamoto and Henderson, 1999), this finding further supports the idea that increased multiple innervation in MHCI-deficient mice is not due to changes in synapse formation, but rather, reflects a disruption of the final stages of synapse elimination.

2.3. Classical MHCIs promote synapse elimination at the developing NMJ

If MHCI promotes synapse elimination, then overexpressing MHCI might accelerate synapse elimination. To test this prediction, we compared multiple innervation at P7, when synapse elimination is not yet complete, in WT mice and in mice that overexpress the mouse MHCI *H-2D*^{b} under the control of the neuron-specific enolase promoter (*NSE-D*^{b} mice; (Rall et al., 1995)). At P7, just over

Please cite this article in press as: Tetruashvily, M.M., et al. MHCI promotes developmental synapse elimination and aging-related synapse loss at the vertebrate neuromuscular junction. Brain Behav. Immun. (2016), http://dx.doi.org/10.1016/j.bbi.2016.01.008

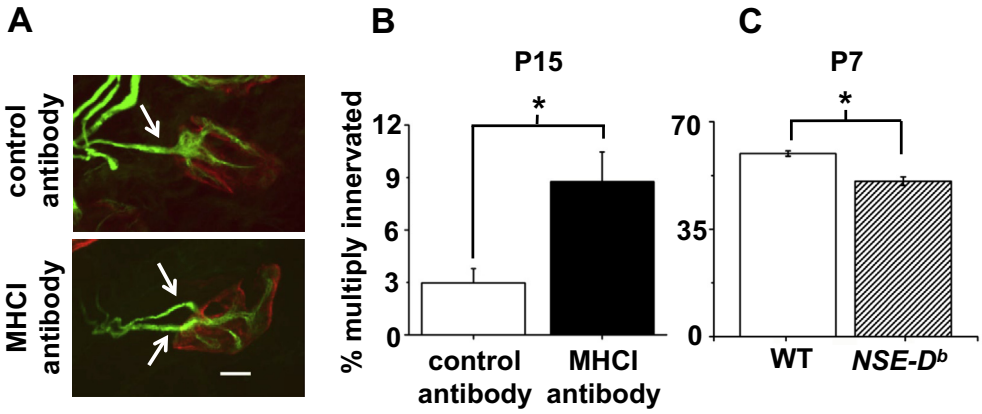


Fig. 2. Anti-MHCI antibodies impair synapse elimination at the NMJ in WT mice, while overexpressing MHCI in neurons accelerates synapse elimination. (A) Representative NMJs from OX18- and IgG1-injected WT animals at P15. nAChRs labeled with α-btx (red); presynaptic axons and terminals labeled with anti-neurofilament and anti-SV2 (green). Arrows, individual MN axons. Scales, 10 μm. (B) Quantification of multiple innervation in IgG1- vs. OX18-injected animals at P15. OX18, 8.8 ± 1.7%; IgG, 3.0 ± 0.8%; $^{*}p = 0.02$. OX18 injection, $n = 9$ animals from 4 litters; IgG1 injection, $n = 6$ animals from 3 litters. (C) At P7, when synapse elimination is not yet complete, there is a modest but significant decrease in the percentage of muscle fibers that remain multiply-innervated in *NSE-D^b* mice, reflecting the fact that postsynaptic sites more rapidly achieve monoinnervation in MHCI-overexpressing animals. WT, $n = 3$; *NSE-D^b*, $n = 5$; $p = 0.012$.

half of postsynaptic sites remain multiply-innervated in WT animals. However, a modestly but significantly lower percentage of postsynaptic sites remained multiply-innervated in MHCI-overexpressing animals (Fig. 2C). The small magnitude of the acceleration may reflect to fact that *H-2D^b* expression is only modestly increased in these transgenics (Lee et al., 2014; Rall et al., 1995). Together, these results demonstrate that developmental synapse elimination at the NMJ can be bi-directionally regulated by changes in MHCI levels: increasing MHCI accelerates synapse elimination, while reducing MHCI disrupts synapse elimination.

These results show that overexpressing just one member of the large MHCI gene family, the classical MHCI *H-2D^b*, is sufficient to accelerate synapse elimination at the NMJ. To determine if classical MHCIs are involved in synapse elimination at the developing NMJ, we examined innervation in $K^{b-/-}D^{b-/-}$ double mutant mice, which lack both of the classical MHCI genes found in C57Bl/6 mice (Vugmeyster et al., 1998). Both *H-2D^b* and *H-2K^b* genes are expressed at the developing NMJ (Tetruashvily et al., in press). At P15, the percentage of multiply-innervated postsynaptic sites was three times WT levels in $K^{b-/-}D^{b-/-}$ mice (multiple innervation 10.6 ± 1.1%, $n = 5$, $p = 0.001$ relative to WT). This was not significantly different from $\beta2m^{-/-}TAP^{-/-}$ values ($p = 0.09$), suggesting that loss of *H-2K* and *H-2D* could fully explain the initial synapse elimination defects in $\beta2m^{-/-}TAP^{-/-}$ mice. In contrast, loss of either *H-2K* or *H-2D* alone did not affect synapse elimination (Fig 1E), suggesting that only a single classical MHCI is necessary for normal synapse elimination to occur. Thus three different models that disrupt MHCI function ($\beta2m^{-/-}TAP^{-/-}$ and $K^{b-/-}D^{b-/-}$ mice, and anti-MHCI function-blocking antibodies injected into WT mice) all cause multiple innervation to persist, together strongly suggesting that MHCI promotes synapse elimination at the developing NMJ. Furthermore, results in *NSE-D^b* and $K^{b-/-}D^{b-/-}$ mice suggest that synapse elimination at the NMJ is promoted by classical MHCI proteins.

2.4. MHCI is expressed at the developing NMJ

MHCI protein is not thought to be expressed in uninjured muscle cells, but has been detected in adult MNs at the NMJ (Thams et al., 2009). mRNAs encoding several MHCI proteins have been detected at the NMJ at multiple ages (Tetruashvily et al., in press). To determine if MHCI protein is present at the NMJ as synapse elimination is occurring, we immunostained intact muscle using a mouse monoclonal antibody (OX-18) that recognizes a monomorphic epitope of rat MHCI (RT-1A (Fukumoto et al., 1982)) and reacts with MHCI from rat, mouse and primate brain in Western blots and immunohistochemistry (Corriveau et al., 1998; Datwani et al., 2009; Dixon-Salazar et al., 2014; Goddard et al., 2007; Huh et al., 2000; Needleman et al., 2010; Rolleke et al., 2006). Several lines of evidence support OX-18's specificity for MHCI in the mouse nervous system (see Section 4). Using OX18, we detect specific MHCI labeling at the NMJ at P7, as synapse elimination is occurring (Fig. S1A). This labeling is abolished by genetic destabilization of MHCI proteins (in $\beta2m^{-/-}TAP^{-/-}$ mice) or by replacing OX-18 with an isotype-control antibody (Fig. S1). Whole-mount muscles were triple-labeled with OX18 to label MHCI, α-btx to label postsynaptic nAChRs, and anti-synaptophysin to visualize presynaptic MN terminals. Because pre- and post-synaptic structures are closely overlaid at the NMJ, three-dimensional reconstruction of staining in confocal Z-stacks is necessary to unambiguously discriminate co-localization with pre- vs. post-synaptic markers. In P7 diaphragm, MHCI co-localizes more extensively in individual optical sections with post-synaptic nAChRs than with presynaptic synaptophysin (Fig. S1A). Specific MHCI labeling does not appear throughout the muscle fiber, but is restricted to the postsynaptic site. Thus MHCI protein is expressed at the NMJ at the time when developmental synapse elimination is occurring.

2.5. Excess MN inputs can be recruited by graded stimulation in MHCI-deficient mice

Surplus MN inputs are functionally silenced before they are physically removed (Colman et al., 1997; Kopp et al., 2000). Our results show that MHCI promotes synapse elimination, but it is unclear if MHCI is involved in only the final physical removal of surplus axons, or is involved in the earlier functional silencing. To discriminate between these possibilities, we performed sharp electrode recordings in P15 WT and MHCI-deficient animals, and applied graded stimulation to the phrenic nerve to sequentially recruit MN inputs (Redfern, 1970). Graded stimulation produced single-amplitude end plate potentials (EPPs) in 100% of recordings from P15 WT animals, as expected, reflecting functional monoinnervation of all postsynaptic sites at this age. In MHCI-deficient animals, in contrast, graded stimulation evoked a large, stepwise increase in the EPP amplitude in 21% of recordings, reflecting

Please cite this article in press as: Tetruashvily, M.M., et al. MHCI promotes developmental synapse elimination and aging-related synapse loss at the vertebrate neuromuscular junction. Brain Behav. Immun. (2016), http://dx.doi.org/10.1016/j.bbi.2016.01.008

recruitment of multiple MN inputs. Multiple inputs could still be recruited at 13% of junctions in MHCI-deficient adults (Fig. 3). These functional measures independently corroborate the anatomical evidence that synapse elimination is impaired in MHCI-deficient mice, and show that some postsynaptic sites continue to receive inputs from MN axons that are distinct all the way to the phrenic nerve, typical of younger animals before synapse elimination is complete (Redfern, 1970; Tapia et al., 2012). Thus persistent multiple innervation in MHCI-deficient animals may result from a failure to silence competing terminal branches, rather than a failure to physically remove silent inputs.

2.6. Increased synaptic strength at MHCI-deficient NMJs

Competing axons develop a disparity in synaptic strength, and weaker inputs are eventually eliminated (Colman et al., 1997; Kopp et al., 2000). Our anatomical and functional data support the idea that MHCI promotes silencing and elimination of MN synapses. In the adult hippocampus, MHCI is required for long-term depression, a form of persistent synaptic weakening (Huh et al., 2000; Nelson et al., 2013). To determine if MHCI is involved in synapse weakening at the developing NMJ, we measured synaptic strength. Quantal size is a measure of synaptic strength that reflects the postsynaptic response to individual quanta of neurotransmitter (Pennefather and Quastel, 1981). At the NMJ, miniature end plate potential (MEPP) amplitude provides a reliable estimate of quantal size (Del Castillo and Katz, 1954). MEPP amplitude is significantly larger than WT in MHCI-deficient animals at P15 ($\beta2m^{-/-}TAP^{-/-}$, 1.78 ± 0.14 mV; WT, 1.15 ± 0.16 mV; $p = 0.022$). Quantal size decreases with age, as previously observed (Wareham et al., 1994), but remains larger in $\beta2m^{-/-}TAP^{-/-}$ adults (P29-P45; $\beta2m^{-/-}TAP^{-/-}$, 1.0 ± 0.08 mV; WT, 0.66 ± 0.06 mV; $p = 0.004$; Fig. S3). Increased quantal size in MHCI-deficient NMJs is not associated with changes in input resistance, EPP decay time, MEPP frequency, paired-pulse facilitation (Fig. S4), postsynaptic nAChR density (Fig. S2), or the number of quanta released per presynaptic nerve impulse (quantal content) (Fig. S4E). Together, these results show that loss of MHCI is associated with an early and persistent increase in synaptic strength. Thus endogenous MHCI promotes synaptic weakening at the developing NMJ, and may contribute to the decline in synaptic strength that precedes functional and physical elimination of competing inputs during normal circuit development (Buffelli et al., 2003; Colman et al., 1997; Kopp et al., 2000).

2.7. MHCI levels rise in aged muscle

MHCI mRNA is up-regulated in aged MNs as they become susceptible to denervation (Edstrom et al., 2004), but is relatively low in MNs that resist aging-related synapse loss (Edstrom et al., 2004; Linda et al., 1999; Valdez et al., 2012). MHCI promotes synapse elimination at the developing NMJ, raising the possibility that higher levels of MHCI could be involved in aging-related muscle denervation. However, elevated mRNA levels do not guarantee increased transcribed protein levels, and to our knowledge, no studies have assessed MHCI protein levels at the aging NMJ. To determine if MHCI protein levels rise at the aging NMJ as denervation is occurring, we compared MHCI expression in extensor digitorum longus (EDL) from P15 and 2-year-old mice using western blotting. The EDL was chosen because it shows significant denervation at this age (Chai et al., 2011; Valdez et al., 2012). Because either H2-K or H2-D are required for developmental synapse elimination (Fig. 1E), we used an antibody (p8) that is specific for H2-K. Values were normalized to a loading control (see Section 4). Comparing MHCI expression in EDL from P15 vs. 2-year-old mice, we found that H2-K levels rise significantly in aging EDL, relative to younger ages (Fig. 4A). Thus MHCI protein is expressed at the NMJ during development, and MHCI levels rise significantly at the aging NMJ.

2.8. MHCI promotes aging-related synapse loss

With aging, synapses are eliminated from mature muscle fibers, leaving some fibers fully denervated (Rudolf et al., 2014; Valdez et al., 2012). We find that during development, MHCI promotes synapse elimination, and MHCI levels rise in aging EDL, raising the possibility that the increase in MHCI expression with age drives aberrant synapse elimination in mature, singly-innervated muscle fibers. To directly test if MHCI contributes to pathological synapse loss in aging muscle, denervation of EDL muscle fibers was assessed in aged (2-year-old) WT and $\beta2m^{-/-}TAP^{-/-}$ mice. Full or partial denervation are evident when postsynaptic nAChRs (labeled with α-btx) are not completely apposed by the nerve terminal, represented by the presynaptic marker SV2 (Valdez et al., 2010). As expected, a subset of muscle fibers were completely denervated in aged EDL (12.2 ± 0.8% fully denervated, $n = 4$). In contrast, both full and partial denervation was dramatically reduced in MHCI-deficient EDL (Fig. 4; full denervation 4.5 ± 1.0%, $p = 0.0009$ relative to WT). While developmental synapse elimination in the EDL was modestly impaired in MHCI-deficient animals (percent multiply-innervated in P15 EDL: WT, 1.0 ± 0.5; $\beta2m^{-/-}TAP^{-/-}$, 5.2 ± 1.1, $n = 3$ animals per age, $p = 0.0045$), this difference is not sufficient to fully explain the reduced denervation in MHCI-deficient EDL. Thus the relative lack of denervation in aged MHCI-deficient animals cannot be fully explained by a different starting point for the aging process, but instead reflects a degree of protection from aging-related denervation. Together, these results show that MHCI levels rise with aging at the NMJ, and that reducing MHCI expression can ameliorate synapse loss in aging muscle.

3. Discussion

Synapse elimination is essential for the establishment of mature neural circuits, while synapse loss later in life is a significant cause of aging-associated pathology. Here we show that MHCI promotes both developmental synapse elimination and aging-related synapse loss at the vertebrate NMJ. MHCI is expressed at the developing NMJ, and three different manipulations that reduce MHCI function-genetic destabilization or deletion of MHCI proteins, or injection of function-blocking anti-MHCI antibodies-cause multiple innervation to persist at otherwise normally-developing synapses. Reducing MHCI expression does not affect patterns of innervation prior to the close of the first postnatal week, suggesting it does not alter earlier synapse formation or elimination. However, synapse elimination during the second week is significantly disrupted, preventing establishment of uniform mono-innervation. Multiply-innervated postsynaptic sites are still present in MHCI-deficient animals at one year of age, are evident both anatomically and functionally, and are associated with increased quantal size. Thus MHCI is required to complete the transition to uniform mono-innervation in developing muscle, and promotes synaptic weakening, one of the earliest hallmarks of competition among multiple inputs to a single muscle fiber. With aging, MHCI levels rise in motor neurons (Edstrom et al., 2004), and in MHCI-deficient mice, aging-related muscle denervation is markedly reduced.

Several experimental conditions delay synapse elimination at the NMJ, including changes in synaptic activity (Misgeld et al., 2002; Thompson et al., 1979), NMDAR activation (Personius et al., 2008), GDNF (Nguyen et al., 1998), BDNF or its receptor TrkB (Je et al., 2013), NCAM (Rafuse et al., 2000), glial neurofascin

Please cite this article in press as: Tetruashvily, M.M., et al. MHCI promotes developmental synapse elimination and aging-related synapse loss at the vertebrate neuromuscular junction. Brain Behav. Immun. (2016), http://dx.doi.org/10.1016/j.bbi.2016.01.008

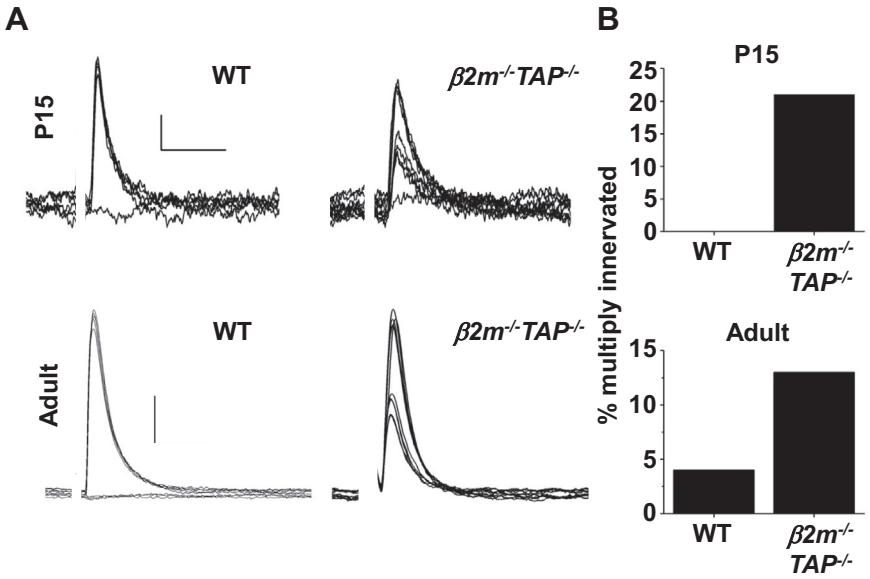


Fig. 3. Multiple functional inputs persist at MHCI-deficient NMJs. (A) Representative EPPs recorded from P15 or adult (P29-45) muscle. Scales: P15, 1 mV, 15 ms; adult, 10 mV, 10 ms. Stimulus artifacts blanked for clarity. (B) Summed electrophysiological data shows increased multiple innervation in MHCI-deficient mice. P15, WT 16 cells from 8 animals, $\beta2m^{-/-}TAP^{-/-}$ 19 cells from 6 animals; adult, WT 25 cells from 5 animals, $\beta2m^{-/-}TAP^{-/-}$ 38 cells from 8 animals.

(Roche et al., 2014), or PKC theta (Li et al., 2004). Synapse elimination is also disrupted in mice which bear a dominant-negative mutation in the *GARS* gene, a mouse model of Charcot-Marie-Tooth type 2D which includes apparent developmental arrest of NMJ maturation (Sleigh et al., 2014). Other manipulations, including increasing activity, reducing gap junctional coupling, or loss of the presynaptic glycine transporter GlyT2, accelerate synapse elimination (Bogdanik et al., 2012; O'Brien et al., 1978; Personius et al., 2007). These and other studies have provided fundamental insights into the molecular and cellular control of the rate of synapse elimination, and suggest factors that may allow synapse elimination to occur normally prior to P7 in MHCI-deficient mice. In some of these models, development of the NMJ is grossly disrupted, which could contribute to their failure to undergo synapse elimination on a normal schedule. While similar gross developmental disruption is not present at MHCI-deficient NMJs, we cannot rule out the possibility that loss of MHCI perturbs synapse elimination indirectly through changes in aspects of development that were not assessed. With most manipulations, however, uniform monoinnervation is still established within the first few postnatal weeks, while multiple innervation is still evident at one year of age in MHCI-deficient mice, suggesting that synapse elimination is persistently disrupted.

We detect MHCI protein at the developing NMJ, where it colocalizes with nAChR labeling, suggesting that it is expressed in the muscle fiber. Importantly, MHCI may also be expressed in the motor neuron and/or Schwann cell during development and/or in aging, a possibility we cannot exclude because there are currently no antibodies to detect most members of the large MHCI family. Multiple MHCI mRNAs are expressed at the NMJ at different ages (Tetruashvily et al., in press). MHCI protein has been detected in presynaptic motor neurons in adult mice (Thams et al., 2009), and in human and rat Schwann cells *in vitro* (Armati et al., 1990; Samuel et al., 1987). Furthermore, we find that modest overexpression of the MHCI H2-D in neurons (Rall et al., 1995) is sufficient to modestly accelerate synapse elimination (Fig. 2C). Ultimately, immuno-electron or super-resolution microscopy, coupled with development of dozens of new antibodies, will be necessary to fully characterize the pre- vs. post-synaptic expression of the many MHCI proteins. Nevertheless, the current results show that MHCI is present at the developing NMJ when synapse elimination is occurring.

MHCI is thought to be repressed by healthy muscle cells, and upregulated only after injury, or in disease states (Karpati et al., 1988). The current results demonstrate an unexpected role for MHCI at the healthy, developing NMJ. Remarkably, MHCI's function at the developing NMJ is strikingly different to its role after injury. Reducing MHCI expression exacerbates loss of synapses made onto axotomized motor neurons (Berg et al., 2013; Oliveira et al., 2004), while we find that both developmental and aging-related loss of motor neuron synapses onto muscles are inhibited.

The bulk of excess MN synapses are pruned prior to P7 (Tapia et al., 2012), but mono-innervation is largely established between P7 and P15, as MNs begin to fire asynchronously (Buffelli et al., 2002; Personius et al., 2001). In MHCI-deficient mice, ~15–20% of postsynaptic sites retain two inputs at P15. No postsynaptic sites received three or more inputs at P15 in MHCI-deficient animals, consistent with the fact that very few postsynaptic sites still receive 3 or more inputs at P7 in WTs (Fig. S2F), the age when MHCI's effects on synapse elimination begin to emerge. The failure of circuit maturation in MHCI-deficient animals is not associated with gross motor defects in mice, but could prevent the emergence of fine-motor control that is behaviorally relevant in humans. Strikingly, the extent of the synapse elimination deficit at the MHCI-deficient NMJ is similar to the extent of axon pruning deficits in the lateral geniculate nucleus of mice lacking MHCI (Datwani et al., 2009; Huh et al., 2000; Lee et al., 2014), or lacking neuron pentraxin (Bjartmar et al., 2006) or components of the complement cascade (Stevens et al., 2007). The reason for the partial nature of the pruning failure in the visual system in these models remains unknown. At the NMJ, however, we find that MHCI is specifically required for the final stages of synapse elimination, during the second postnatal week (Fig. 1). In adult motor neurons, levels of the classical MHCI H-2D appear to be heterogeneous (Thams et al., 2009), raising the possibility that different levels of MHCI during development may also render some inputs more susceptible to elimination. Alternatively other factors, including fiber type and associated activity patterns, may influence the role that

Please cite this article in press as: Tetruashvily, M.M., et al. MHCI promotes developmental synapse elimination and aging-related synapse loss at the vertebrate neuromuscular junction. Brain Behav. Immun. (2016), http://dx.doi.org/10.1016/j.bbi.2016.01.008

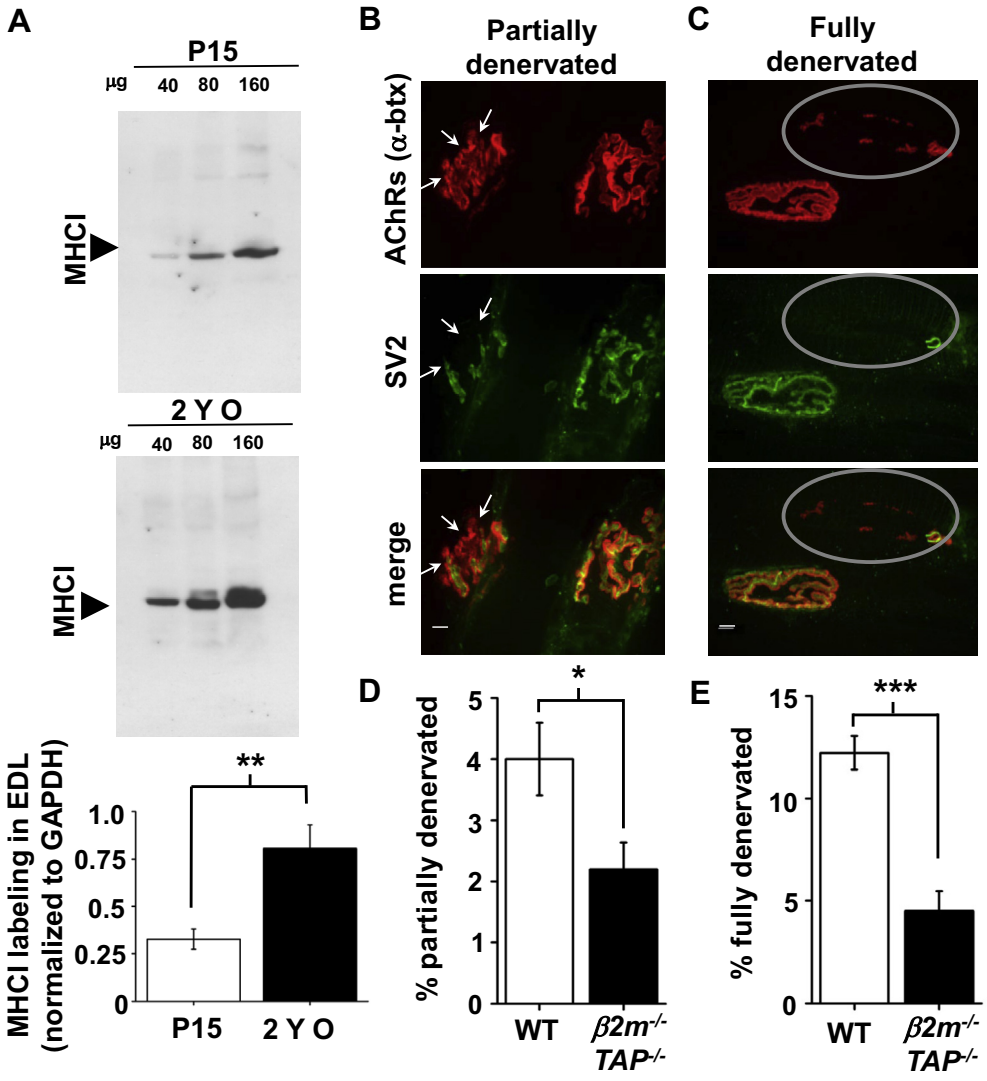


Fig. 4. MHCI protein levels climb in aging EDL, and reducing MHCI expression prevents aging-related denervation. (A) Western blots for MHCI in lysates of EDL muscle from P15 and 2-year-old mice. Three different total protein concentrations are shown. Blots were stripped and probed for GAPDH as a loading control. Bottom, MHCI densitometry normalized to GAPDH for six technical replicates (two per concentration) at each age. $p = 0.0048$. (B, C) EDL muscles from 24–26 month-old mice were stained with α-btx (red) to detect nAChRs and SV2 (green) to detect presynaptic nerve terminals. Representative images show examples of partially (arrows, B) and fully (oval, C) denervated AChR clusters in WT EDL (red with no associated green in merge). Scales, 7 μm. (D, E) Mean partial (D) and full (E) denervation in 2 year old EDL muscle from WT and MHCI-deficient $\beta2m^{-/-}TAP^{-/-}$ mice ($n = 4$ per genotype). $^{*}p = 0.03$; $^{***}p = 0.0009$.

MHCI plays in elimination of specific axon branches. This is consistent with the finding that MHCI is required for synapse elimination to reach completion in the diaphragm, which consists of a mixture of fast and slow fiber types, but has a smaller influence on synapse elimination in the EDL, which is almost exclusively composed of fast-twitch fibers (Eddinger et al., 1985). Together, the current results suggest that synapse elimination at the NMJ may be divided into stages with distinct molecular requirements, and that MHCI is essential as the last postsynaptic sites transition from dual- to mono-innervation.

During synapse elimination at the NMJ, competing axons develop a disparity in synaptic strength which precedes withdrawal of the weaker input (Colman et al., 1997; Kopp et al., 2000). While it is unknown if larger synaptic strength at the MHCI-deficient NMJ is related to deficits in synapse elimination, stronger inputs may be less vulnerable to competition-induced synaptic weakening. In this way, loss of MHCI might prevent the development of sufficient disparity in synaptic strength to trigger functional silencing and physical elimination in the most closely-matched competitions. Interestingly, paired increases in synapse strength and density like those we observe at the MHCI-deficient NMJ are also seen in the cortex (Glynn et al., 2011) and lateral geniculate nucleus (LGN) (Lee et al., 2014) of MHCI-deficient mice. Additional studies in MHCI-deficient mice found increases in synapse density in cortex (Adelson et al., 2014), and increased synapse density (Dixon-Salazar et al., 2014) and strength (Fourgeaud et al., 2010) in hippocampus. While the present study identifies a role for MHCI in synapse elimination at the NMJ, it is as yet unknown if MHCI inhibits synapse formation and/or promotes synapse elimination in cortex or hippocampus.

It will be important to determine if MHCI expression is regulated by activity at the developing NMJ, as it is in the visual system (Corriveau et al., 1998), to determine if it is specifically responsive to the levels, patterns, and/or synchronization of activity, and to fully define the cellular and molecular networks linking MHCI to changes in the strength and connectivity of synapses. An immunoreceptor for MHCI, PirB, has been detected in the CNS (Syken et al., 2006), and at the adult NMJ (Thams et al., 2009),

Please cite this article in press as: Tetruashvily, M.M., et al. MHCI promotes developmental synapse elimination and aging-related synapse loss at the vertebrate neuromuscular junction. Brain Behav. Immun. (2016), http://dx.doi.org/10.1016/j.bbi.2016.01.008

but knocking out PirB does not replicate the failure of retinogeniculate pruning seen in MHCI-deficient mice (Datwani et al., 2009; Huh et al., 2000; Lee et al., 2014; Syken et al., 2006), suggesting that in the retino-geniculate projection, MHCI promotes developmental synapse elimination via a PirB-independent mechanism. It remains an open question whether PirB is involved in MHCI-dependent changes in synapse number at the NMJ, or in other regions of the CNS, such as hippocampus and cortex. Overall, a detailed molecular mechanistic understanding of MHCI signaling in the nervous system is still lacking. The current study opens the door to advance this critical research at the NMJ, a large, accessible synapse that is uniquely amenable to manipulation and imaging *in vivo*.

In MHCI-deficient animals, aging-related denervation of EDL muscle fibers is decreased. The characteristic fragmentation or absence of pre- and/or post-synaptic staining at some NMJs in aged animals is unlikely to be due to incomplete labeling, for several reasons: (1) similar discontinuities are never observed in younger muscle; (2) in 2-year-old muscle, most postsynaptic sites are fully labeled; and (3) the percentage of denervated muscle fibers measured in WTs corresponds well with published values for this muscle (e.g., (Chai et al., 2011; Valdez et al., 2012)). The relative absence of denervation in MHCI-deficient animals cannot be fully explained by the persistence of supernumary inputs and preferential loss of these excess inputs with aging, because developmental synapse elimination, while impaired, is still largely complete at P15 in the EDL in MHCI-deficient animals.

In adults, MHCI levels increase in situations where muscle fiber denervation occurs, including nerve injury, neuromuscular disorders, and normal aging (Edstrom et al., 2004; Emslie-Smith et al., 1989; Thams et al., 2009). MHCI expression is notably low in MNs innervating the extra-ocular muscles (EOMs) (Linda et al., 1999), which are resistant to aging-associated denervation (Valdez et al., 2012). Here we provide evidence that MHCI protein levels rise at the aging NMJ, and that MHCI promotes denervation of aging muscle. Recent studies also identified a role for MHCI and the MHCI light chain, β2m, in cognitive aging (Smith et al., 2015). While we find that MHCI is selectively required for the final stages of synapse elimination at the developing NMJ, denervation of aging muscle is almost completely prevented in MHCI-deficient mice, suggesting that vulnerability to aging-related denervation largely depends on MHCI. Together, the current results show that MHCI promotes weakening and elimination of surplus synapses at the developing NMJ, and suggest that aberrant reactivation of MHCI-dependent synapse elimination mechanisms may contribute to pathological denervation of adult muscle. They also identify MHCI as a therapeutic target for the prevention of aging-related motor impairments.

4. Materials and methods

4.1. Animal subjects

All experimental protocols were conducted according to the National Institutes of Health (NIH) guidelines for animal research and approved by the Institutional Animal Care and Use Committee (IACUC) at the University of California, San Diego and/or Princeton University. The following mouse strains were used: (1) C57B1/6 wild-type (WT, Harlan/Jackson Labs); (2) mice lacking expression of the MHCI light chain, *β2m*, as well as the transporter for antigen processing, *TAP1*, which show greatly reduced stable cell-surface expression of most, but not all, MHCI proteins ($\beta 2m^{-/-}TAP^{-/-}$, courtesy of D. Raulet and C.J. Shatz) (Dorfman et al., 1997; Ljunggren et al., 1995); (3) mice which 1.2.8 and lack expression of both of the classical MHCI genes present in C57Bl/6, *H-2K* and *H-2D* ($K^{b-/-}D^{b-/-}$, courtesy of C.J. Shatz) (Vugmeyster et al., 1998); (4) mice which lack expression of single classical MHCI genes *H-2K* or *H-2D* ($K^{b-/-}$ and $D^{b-/-}$, Taconic) (Perarnau et al., 1999) and (5) mice which overexpress the classical MHCI $H\text{-}2D^b$ under the control of the neuron-specific enolase promoter ($NSE\text{-}D^b$, courtesy of M.B.A. Oldstone) (Rall et al., 1995).

4.2. Visualization of neuromuscular junctions using immunohistochemistry and rhodamine-conjugated α-bungarotoxin (α-btx)

Whole mounts of mouse diaphragm muscle were immunostained at P0, P7, P15, P29-50, 12–13 months, or 22–24 months, and mouse EDL was stained at P15 and 22–24 months. Animals were deeply anesthetized using inhaled isoflurane and tissue was drop-fixed with 4% PFA (Electron Microscopy Systems) in phosphate buffered saline (PBS, Sigma) for 30 min. Diaphragm and EDL muscles were dissected, rinsed in PBS, incubated in 0.1% glycine (Fischer) for 12 h at 4 °C and then blocked in a solution containing 3% goat serum albumin (GSA, Jackson) and 0.1% Triton X-100 in PBS for 12 h at 4 °C, both on rockers. Presynaptic MN terminals were visualized by treating muscles for 48–72 h at 4 °C with a primary antibody cocktail consisting of one or both of the following: anti-neurofilament (Invitrogen, 1:500) and anti-SV2 (developed by K. M. Buckley under the auspices of the NICHD, maintained by The University of Iowa Department of Biology, obtained from the Developmental Studies Hybridoma Bank, 1:100). Tissues were rinsed in PBS for 3x2hrs and then incubated in Alexa-488-conjugated goat anti-mouse IgG (Jackson, 1:100) for 18–24 h at 4 °C. Tissues were rinsed in PBS for 3 × 2 h and treated with rhodamine-conjugated α-btx (Molecular Probes, 10 μg/100 μL) to label postsynaptic nicotinic acetylcholine receptors for 30 min. After a final rinse in PBS, tissues were mounted on slides using fluorescence-stabilizing mounting media (Vectashield hard set mount) and microscopy was performed using a Leica (Wetzlar, Germany) DMI6000 inverted microscope outfitted with a Yokogawa (Tokyo, Japan) spinning disk confocal head and an Orca ER high resolution B&W cooled CCD camera (Hamamatsu, Sewickley, PA). This approach yielded robust immunostaining that allowed clear discrimination of motor neuron axons and presynaptic motor end plates. To ensure maximal antibody penetration, we examined surface fibers at approximately the same depth in all tissues.

Importantly, the appearance of presynaptic immunofluorescence is expected to differ qualitatively from presynaptic fluorescence in mouse lines expressing YFP in a subset of motor neurons, which have been used in many influential studies of the development and denervation of the NMJ (e.g., (Valdez et al., 2010)). This is because antibodies gradually penetrate the tissue to label specific presynaptic structures (SV2, synaptic vesicles; NF, neurofilament), while YFP is a soluble protein that, when overexpressed in motor neurons, diffuses throughout the presynaptic cytoplasm.

To assess multiple innervation, montages of Z-serial images (<20 μm total thickness per junction) were collected from intact muscles under a 63× oil immersion lens at 1.6× magnification. Z-stacks of at least 50 terminals from each hemidiaphragm or EDL muscle (two per animal; each animal was considered an independent *n*) were examined from each animal at each age by an observer blind to genotype. Junctions were uniformly sampled over the entire dorsal–ventral axis. Innervation was assessed by counting the number of anatomically distinct MN axons contacting each postsynaptic junction, by tracing them back as far as possible in unflattened confocal stacks (5.4–27 μm total depth). In most cases preterminal axons could be followed 50–100 μm from the synapse. Examination of unflattened confocal Z-stacks from multiple depths and angles is necessary to unambiguously distinguish individual MN axons innervating a single postsynaptic site, and

Please cite this article in press as: Tetruashvily, M.M., et al. MHCI promotes developmental synapse elimination and aging-related synapse loss at the vertebrate neuromuscular junction. Brain Behav. Immun. (2016), http://dx.doi.org/10.1016/j.bbi.2016.01.008

to determine if two axons innervate one postsynaptic site, or simply two postsynaptic sites in different focal planes. Junctions in which multiple innervation could not be unambiguously determined (e.g., due to extensive axon fasciculation, variation in labeling intensity, proximity of other nAChR clusters, or depth of axons) were scored as monoinnervated, to ensure a conservative estimate of multiple innervation. Postsynaptic perimeter and area were assessed and quantified using ImageJ software (NIH).

For denervation studies in aged EDL, montages of Z-serial images (<20 μm total thickness per junction) were collected from intact muscles under a 63× oil immersion lens at 1.6× magnification. Z-stacks of at least 50 terminals from each EDL (two EDLs per animal; each animal was considered an independent *n*) were examined from each animal by an observer blind to genotype. Junctions were uniformly sampled over the entire muscle. Innervation of a muscle fiber was defined as colocalization of green, SV2-labeled presynaptic axon terminals with α-btx-labeled postsynaptic nAChRs. Both partial and full denervation were scored, as identified as nAChR labeling not fully apposed to presynaptic SV2 labeling, the same criteria used in (Valdez et al., 2010) (Fig. 4). Most denervated NMJs also showed one or more additional aging-associated changes, including: (1) nAChR fragmentation (>5 nAChR islands; abnormal nAChR cluster shape) and decreased nAChR density (noticeably dimmer α-btx labeling compared to other muscle fibers in the same confocal plane); (2) retraction of the MN axon, multiple innervation, and extra-junctional MN sprouting; and (3) axonal varicosities proximal to the NMJ and axonal atrophy (thinning of the preterminal or terminal axon).

4.3. MHCI and synaptophysin immunohistochemistry

Anesthetized P7 WT and $\beta2m^{-/-}TAP^{-/-}$ animals were perfused transcardially with 4% PFA. Diaphragms were dissected and stored at 4 °C overnight. Muscles were cleaned of connective tissue and blocked in a solution containing 5% bovine serum albumin, 0.01% Triton X-100 and 0.1% sodium azide (Fischer) for one hour. Muscles were treated with primary antibodies against synaptophysin (SYPH, Santa Cruz, 1:100) and MHCI (OX18, AbdSerotec, 1:100) overnight at 4 °C. OX18 is a mouse monoclonal antibody that recognizes a monomorphic epitope in the α3 region of the rat MHCI RT-1A (Fukumoto et al., 1982), and reacts with mouse MHCI in Western blots and immunohistochemistry (Corriveau et al., 1998; Datwani et al., 2009; Dixon-Salazar et al., 2014; Goddard et al., 2007; Huh et al., 2000). The suspected mouse orthologue of rat RT-1A, H-2K1, is 84.9% identical and 89.2% similar to RT-1A at the amino acid level in the α3 region, the site of the OX-18 epitope. Several lines of evidence support OX-18's ability to bind to MHCI in the mouse nervous system. First, genetically deleting the MHCI light chain, β2m, reduces the amount of MHCI that reaches the cell surface (Dorfman et al., 1997; Zijlstra et al., 1989), and cell surface OX-18 immunofluorescence is greatly attenuated in both $\beta2m^{-/-}$ (Needleman et al., 2010) and $\beta2m^{-/-}TAP^{-/-}$ (Goddard et al., 2007) neurons *in vitro*. Second, OX-18 recognizes proteins of the expected molecular weight in western blots of adult mouse brain (Corriveau et al., 1998; Dixon-Salazar et al., 2014; Huh et al., 2000) and similar labeling is seen in rat brain using a rabbit polyclonal antibody that recognizes a distinct epitope of MHCI (Needleman et al., 2010). The secondary antibodies we used to detect MHCI cause some nonspecific background labeling, which can be clearly distinguished from specific labeling in two ways: (1) it is still present when labeling with an isotype-control antibody, and (2) it is not abolished in MHCI-deficient animals (Fig. S1). Using these criteria, specific MHCI labeling is present at the postsynaptic site, while other muscle labeling is nonspecific. Taken together, these results provide strong support for the specificity of OX-18 in recognizing MHCI at the mouse NMJ.

Incubation in primary antibody was followed by 3 × 40 min rinses in PBS, and a four hour treatment with the appropriate cocktail of Alexa-488-conjugated donkey anti-mouse IgG (Invitrogen, 1:1000) and/or Cy5-conjugated donkey anti-goat IgG (Jackson, 1:100) in block. After rinsing 3 × 40 min, muscles were treated for 30 min with rhodamine-conjugated α-bungarotoxon (α-btx) diluted 1:10 in ddH_2O. Samples were rinsed in 3 × 20 min in PBS, mounted on glass slides, and coverslipped using Vectashield hardset mount. Coverslipped slides were sandwiched between two pieces of paper towel and compressed under a lead brick overnight, edges sealed with clear nail polish, and stored at 4 °C until imaging. Z-serial images (0.5 μm per step, up to 20 μm total depth per junction) were collected from intact muscles using a Leica (Wetzlar, Germany) DMI6000 inverted microscope outfitted with a Yokogawa (Tokyo, Japan) spinning disk confocal head and an Orca ER high resolution B&W cooled CCD camera (Hamamatsu, Sewickley, PA) under a 63× oil immersion lens at 1.6× magnification. WT and $\beta2m^{-/-}TAP^{-/-}$ samples were imaged under identical conditions during the same microscopy session.

4.4. Western blotting

EDL muscles were dissected as above from P15 and aged (2 year old) WT mice (2 animals per age). Pooled tissue for each age was suspended in 500 μl of lysis buffer (50 mM NaH_2PO_4, 300 mM NaCl, 10 mM imidazole, 1% NP-40, 0.5% TritonX-100, Halt protease and phosphatase inhibitor (Pierce, Rockland, IL) and flash-frozen in liquid nitrogen. Frozen tissue was placed in pre-cooled 50 ml grinding jars along with a 20 mm stainless steel ball bearing and subjected to cryogenic grinding in liquid nitrogen for 20 min at 25 Hz on a Retsch CryoMill until rendered into a fine powder. Total protein concentration in the samples was determined using a NanoDrop ND-1000 UV–Vis spectrophotometer from Thermo (absorbance (A280) was measured). Samples (40, 80, or 160 μg/lane) were subjected to SDS–PAGE using 4–20% Mini-PROTEAN® TGX™ gradient gels from BIORAD, and transferred to a PVDF membrane.

Membranes were blocked for 1 h at room temperature (RT; ~25 °C) in 5% organic dry milk in TBST. Primary antibodies (anti-MHCI [p8, 1:500, purified rabbit polyclonal raised against exon 8 of H-2K, GeneScript] or anti-GAPDH [MAB374, 1:5,000, purified mouse monoclonal raised against rabbit GAPDH, EMD Millipore]) were diluted in blocking buffer and incubated with the membranes overnight at 4 °C (p8) or 1 h at RT (GAPDH). Membranes were washed 12 × 5 min in TBST, followed by 1 h incubation at RT with the appropriate HRP-conjugated secondary antibody (for MHCI: goat anti-rabbit HRP [1:5,000] from Jackson ImmunoResearch Laboratories, product #111:035:144; for GAPDH: goat anti-mouse HRP [1:10,000] from ThermoFisher, product #A24512). Membranes were washed 12 × 5 min in TBST and labeling detected using either Pierce ECL Western Blotting Substrate (Pierce, Rockland, IL catalog # 32106) (for GAPDH) or SuperSignal West Pico Chemiluminescent Substrate (Pierce, Rockland, IL catalog # 34080) (for MHCI) and used to expose HyBlot CL Autoradiography Film (Denville Scientific, Metuchen, NJ). Blots were first probed for MHCI, and then stripped and reprobed for GAPDH. Blots were stripped using a mild stripping solution (1L of water containing 15 g glycine, 1 g SDS, 10 ml Tween 20, pH 2.2) heated to 55 °C. Blots were incubated in 20 ml of stripping solution for 10 min, washed 12 × 5 min in TBST, and blocked and processed as above for the second antibody (anti-MHCI).

4.5. Electrophysiology

Hemidiaphragm-phrenic nerve preparations were used from WT and $\beta2m^{-/-}TAP^{-/-}$ animals at P14-16 and adult (P29-P45) ages. Muscles were dissected from anesthetized animals under cold,

Please cite this article in press as: Tetruashvily, M.M., et al. MHCI promotes developmental synapse elimination and aging-related synapse loss at the vertebrate neuromuscular junction. Brain Behav. Immun. (2016), http://dx.doi.org/10.1016/j.bbi.2016.01.008

oxygenated (95% CO_2/5% O_2) Rees normal mammalian ringers (NMR; (Rees, 1978)) consisting of (in mM): 135 NaCl, 5 KCl, 15 $NaHCO_3$, 1 Na_2HPO_4, 1 $MgSO_4$, 2.5 Ca gluconate, and 11 glucose, pH 7.4. Contraction blockade, which is necessary to permit microelectrode recordings from postsynaptic muscle fibers, was achieved via 1 h pretreatment of diaphragms in oxygenated 2 μM μ-conotoxin (Bachem) (adult muscles) or 3–6 μM tubocurare (P15). Muscles were pinned to a Sylgard-lined recording chamber and superfused (1 mL/min) with oxygenated NMR at 22–24 °C. Intracellular recordings of muscles fibers were performed using sharp recording electrodes (30–69 MΩ) filled with 3 M KCl. End plate potentials (EPPs) were evoked via suprathreshold stimulation of the phrenic nerve with a suction electrode (square pulses, 0.2 ms duration at 0.5 Hz). Electrodes were visually guided to NMJs under oblique illumination. Responses with rise times of more than 1.5 ms represent electrode placements relatively distant from the junction, and were discarded. Membrane potentials were continuously recorded and only muscle fibers in which potentials were <−55 mV and stable within ±5 mV were included in analysis. Membrane responses were amplified by an Axoclamp 2A amplifier (Axon Instruments), low-pass filtered at 1 kHz, and digitized and recorded using WinWCP software (John Dempster).

Levels of innervation were assessed electrophysiologically by applying graded stimulation to the phrenic nerve stump and counting the number of elicited inputs of differential amplitude above normal quantal variability. Miniature end-plate potentials (MEPPS) were recorded in gap-free mode from singly-innervated junctions and analyzed offline using MiniAnalysis software (Justin Lee; Synaptosoft). For quantal content analysis, EPPS were evoked and MEPPs were recorded for two seconds following stimulation at singly-innervated junctions. Quantal content was estimated as the ratio of the mean EPP amplitude to the mean MEPP amplitude (Wood and Slater, 2001).

4.6. Antibody injections

P7 WT mice received daily intraperitoneal injections for 7 days with 10 μg/g body weight of either panspecific anti-MHCI antibody (OX18; AbdSerotec) or isotype-matched mouse IgG1 control (AbdSerotec). While injecting one specific antibody against H-2^d, can induce a model of transfusion-induced lung injury in rats (Looney et al., 2006), nine other anti-MHCI antibodies, including OX18, do not induce this model (Kelher et al., 2009; Strait et al., 2011). P15 mice were perfused and diaphragms were either immunostained for neuromuscular morphology as described above, or treated with Alexa 488-conjugated goat anti-mouse IgG1 (Invitrogen, 1:100) for four hours to visualize OX18 or IgG1 binding.

4.7. Data analysis

All immunohistochemical experiments were collected and analyzed blind to genotype. Data are presented as mean ± standard error of the mean. p Values determined by unpaired one-tailed Student's t-test. Unless otherwise noted, asterisks indicate $p < 0.05$, and n = number of animals.

Acknowledgments

We thank E. O'Driscoll, K. K. Frietze, R. Wyatt and J.J. Park for technical support, R. Balice-Gordon for protocols and discussion, G. Patrick and M. Scanziani for loaned equipment, D. Raulet and C. Shatz for transgenic mice, and A. Ghosh and C. Tyler for comments. Electrophysiological experiments piloted in UCSD Teaching Labs with L. Lopez. Supported by 1F30AG046044-01A1, the Princeton Department of Molecular Biology and the Princeton Neuroscience Institute (M.M.T), the UCSD School of Medicine (M.A.M.), the New Jersey Commission on Brain Injury Research (K.K.F.), the Alfred P. Sloan Foundation, the Whitehall Foundation, and a Princeton Neuroscience Institute Innovation Award (L.M.B.).

Appendix A. Supplementary data

Supplementary data associated with this article can be found, in the online version, at http://dx.doi.org/10.1016/j.bbi.2016.01.008.

References

Adelson, J.D., Barreto, G.E., Xu, L., Kim, T., Brott, B.K., Ouyang, Y.B., Naserke, T., Djurisic, M., Xiong, X., Shatz, C.J., et al., 2012. Neuroprotection from stroke in the absence of MHCI or PirB. Neuron 73, 1100–1107, S0896-6273(12)00138-9 [pii] 10.1016/j.neuron.2012.01.020.

Adelson, J.D., Sapp, R.W., Brott, B.K., Lee, H., Miyamichi, K., Luo, L., Cheng, S., Djurisic, M., Shatz, C.J., 2014. Developmental sculpting of intracortical circuits by MHC Class I H2-Db and H2-Kb. Cereb Cortex. http://dx.doi.org/10.1093/cercor/bhu243.

Armati, P.J., Pollard, J.D., Gatenby, P., 1990. Rat and human Schwann cells in vitro can synthesize and express MHC molecules. Muscle Nerve 13, 106–116. http://dx.doi.org/10.1002/mus.880130204.

Berg, A., Zelano, J., Thams, S., Cullheim, S., 2013. The extent of synaptic stripping of motoneurons after axotomy is not correlated to activation of surrounding glia or downregulation of postsynaptic adhesion molecules. PLoS One 8, e59647. http://dx.doi.org/10.1371/journal.pone.0059647.

Bjartmar, L., Huberman, A.D., Ullian, E.M., Renteria, R.C., Liu, X., Xu, W., Prezioso, J., Susman, M.W., Stellwagen, D., Stokes, C.C., et al., 2006. Neuronal pentraxins mediate synaptic refinement in the developing visual system. J. Neurosci. 26, 6269–6281. http://dx.doi.org/10.1523/JNEUROSCI.4212-05.2006.

Blom, W.M., De Bont, H.J., Meijerman, I., Kuppen, P.J., Mulder, G.J., Nagelkerke, J.F., 1999. Interleukin-2-activated natural killer cells can induce both apoptosis and necrosis in rat hepatocytes. Hepatology 29, 785–792, S0270913999001202 [pii] 10.1002/hep.510290303.

Bogdanik, L.P., Chapman, H.D., Miers, K.E., Serreze, D.V., Burgess, R.W., 2012. A MusD retrotransposon insertion in the mouse Slc6a5 gene causes alterations in neuromuscular junction maturation and behavioral phenotypes. PLoS One 7, e30217. http://dx.doi.org/10.1371/journal.pone.0030217 PONE-D-11-20438 [pii].

Brown, M.C., Jansen, J.K., Van Essen, D., 1976. Polyneuronal innervation of skeletal muscle in new-born rats and its elimination during maturation. J Physiol 261, 387–422.

Buffelli, M., Busetto, G., Cangiano, L., Cangiano, A., 2002. Perinatal switch from synchronous to asynchronous activity of motoneurons: link with synapse elimination. Proc Natl Acad Sci U S A 99, 13200–13205. http://dx.doi.org/10.1073/pnas.202471199.

Buffelli, M., Burgess, R.W., Feng, G., Lobe, C.G., Lichtman, J.W., Sanes, J.R., 2003. Genetic evidence that relative synaptic efficacy biases the outcome of synaptic competition. Nature 424, 430–434. http://dx.doi.org/10.1038/nature01844 nature01844 [pii].

Busetto, G., Buffelli, M., Tognana, E., Bellico, F., Cangiano, A., 2000. Hebbian mechanisms revealed by electrical stimulation at developing rat neuromuscular junctions. J. Neurosci. 20, 685–695.

Chai, R.J., Vukovic, J., Dunlop, S., Grounds, M.D., Shavlakadze, T., 2011. Striking denervation of neuromuscular junctions without lumbar motoneuron loss in geriatric mouse muscle. PLoS One 6, e28090. http://dx.doi.org/10.1371/journal.pone.0028090 PONE-D-11-11057 [pii].

Colman, H., Nabekura, J., Lichtman, J.W., 1997. Alterations in synaptic strength preceding axon withdrawal. Science 275, 356–361.

Corriveau, R.A., Huh, G.S., Shatz, C.J., 1998. Regulation of class I MHC gene expression in the developing and mature CNS by neural activity. Neuron 21, 505–520.

Datwani, A., McConnell, M.J., Kanold, P.O., Micheva, K.D., Busse, B., Shamloo, M., Smith, S.J., Shatz, C.J., 2009. Classical MHCI molecules regulate retinogeniculate refinement and limit ocular dominance plasticity. Neuron 64, 463–470, S0896-6273(09)00844-7 [pii] 10.1016/j.neuron.2009.10.015.

Del Castillo, J., Katz, B., 1954. Quantal components of the end-plate potential. J Physiol 124, 560–573.

Dixon-Salazar, T.J., Fourgeaud, L., Tyler, C.M., Poole, J.R., Park, J.J., Boulanger, L.M., 2014. MHC class I limits hippocampal synapse density by inhibiting neuronal insulin receptor signaling. J. Neurosci. 34, 11844–11856. http://dx.doi.org/10.1523/JNEUROSCI.4642-12.2014.

Dorfman, J.R., Zerrahn, J., Coles, M.C., Raulet, D.H., 1997. The basis for self-tolerance of natural killer cells in beta2-microglobulin- and TAP-1- mice. J. Immunol. 159, 5219–5225.

Eddinger, T.J., Moss, R.L., Cassens, R.G., 1985. Fiber number and type composition in extensor digitorum longus, soleus, and diaphragm muscles with aging in Fisher 344 rats. J. Histochem. Cytochem. 33, 1033–1041.

Edstrom, E., Kullberg, S., Ming, Y., Zheng, H., Ulfhake, B., 2004. MHC class I, beta2 microglobulin, and the INF-gamma receptor are upregulated in aged motoneurons. J. Neurosci. Res. 78, 892–900.

Emslie-Smith, A.M., Arahata, K., Engel, A.G., 1989. Major histocompatibility complex class I antigen expression, immunolocalization of interferon subtypes, and T cell-mediated cytotoxicity in myopathies. Hum. Pathol. 20, 224–231.

Fourgeaud, L., Davenport, C.M., Tyler, C.M., Cheng, T.T., Spencer, M.B., Boulanger, L. M., 2010. MHC class I modulates NMDA receptor function and AMPA receptor trafficking. Proc. Natl. Acad. Sci. USA 107, 22278–22283, 0914064107 [pii] 10.1073/pnas.0914064107.

Fukumoto, T., McMaster, W.R., Williams, A.F., 1982. Mouse monoclonal antibodies against rat major histocompatibility antigens. Two Ia antigens and expression of Ia and class I antigens in rat thymus. Eur. J. Immunol. 12, 237–243.

Glynn, M.W., Elmer, B.M., Garay, P.A., Liu, X.B., Needleman, L.A., El-Sabeawy, F., McAllister, A.K., 2011. MHCI negatively regulates synapse density during the establishment of cortical connections. Nat. Neurosci. 14, 442–451, nn.2764 [pii] 10.1038/nn.2764.

Goddard, C.A., Butts, D.A., Shatz, C.J., 2007. Regulation of CNS synapses by neuronal MHC class I. Proc Natl Acad Sci U S A 104, 6828–6833.

Hayashi-Takagi, A., Araki, Y., Nakamura, M., Vollrath, B., Duron, S.G., Yan, Z., Kasai, H., Huganir, R.L., Campbell, D.A., Sawa, A., 2014. PAKs inhibitors ameliorate schizophrenia-associated dendritic spine deterioration in vitro and in vivo during late adolescence. Proc Natl Acad Sci U S A 111, 6461–6466. http://dx.doi.org/10.1073/pnas.1321109111.

Hedden, T., Gabrieli, J.D., 2004. Insights into the ageing mind: a view from cognitive neuroscience. Nat. Rev. Neurosci. 5, 87–96. http://dx.doi.org/10.1038/nrn1323.

Huh, G.S., Boulanger, L.M., Du, H., Riquelme, P.A., Brotz, T.M., Shatz, C.J., 2000. Functional requirement for class I MHC in CNS development and plasticity. Science 290, 2155–2159.

Je, H.S., Yang, F., Ji, Y., Potluri, S., Fu, X.Q., Luo, Z.G., Nagappan, G., Chan, J.P., Hempstead, B., Son, Y.J., et al., 2013. ProBDNF and Mature BDNF as Punishment and Reward Signals for Synapse Elimination at Mouse Neuromuscular Junctions. J. Neurosci. 33, 9957–9962, 33/24/9957 [pii] 10.1523/JNEUROSCI.0163-13.2013.

Karpati, G., Pouliot, Y., Carpenter, S., 1988. Expression of immunoreactive major histocompatibility complex products in human skeletal muscles. Ann. Neurol. 23, 64–72. http://dx.doi.org/10.1002/ana.410230111.

Kelher, M.R., Masuno, T., Moore, E.E., Damle, S., Meng, X., Song, Y., Liang, X., Niedzinski, J., Geier, S.S., Khan, S.Y., et al., 2009. Plasma from stored packed red blood cells and MHC class I antibodies causes acute lung injury in a 2-event in vivo rat model. Blood 113, 2079–2087. http://dx.doi.org/10.1182/blood-2008-09-177857.

Keller-Peck, C.R., Walsh, M.K., Gan, W.B., Feng, G., Sanes, J.R., Lichtman, J.W., 2001. Asynchronous synapse elimination in neonatal motor units: studies using GFP transgenic mice. Neuron 31, 381–394, S0896-6273(01)00383-X [pii].

Kopp, D.M., Perkel, D.J., Balice-Gordon, R.J., 2000. Disparity in neurotransmitter release probability among competing inputs during neuromuscular synapse elimination. J. Neurosci. 20, 8771–8779.

Krey, J.F., Pasca, S.P., Shcheglovitov, A., Yazawa, M., Schwemberger, R., Rasmusson, R., Dolmetsch, R.E., 2013. Timothy syndrome is associated with activity-dependent dendritic retraction in rodent and human neurons. Nat. Neurosci. 16, 201–209, nn.3307 [pii] 10.1038/nn.3307.

Lee, Y.I., Mikesh, M., Smith, I., Rimer, M., Thompson, W., 2011. Muscles in a mouse model of spinal muscular atrophy show profound defects in neuromuscular development even in the absence of failure in neuromuscular transmission or loss of motor neurons. Dev. Biol. 356, 432–444, S0012-1606(11)00982-1 [pii] 10.1016/j.ydbio.2011.05.667.

Lee, H., Brott, B.K., Kirkby, L.A., Adelson, J.D., Cheng, S., Feller, M.B., Datwani, A., Shatz, C.J., 2014. Synapse elimination and learning rules co-regulated by MHC class I H2-D. Nature 509, 195–200. http://dx.doi.org/10.1038/nature13154.

Letellier, M., Willson, M.L., Gautheron, V., Mariani, J., Lohof, A.M., 2008. Normal adult climbing fiber monoinnervation of cerebellar Purkinje cells in mice lacking MHC class I molecules. Dev. Neurobiol. 68, 997–1006.

Li, M.X., Jia, M., Yang, L.X., Jiang, H., Lanuza, M.A., Gonzalez, C.M., Nelson, P.G., 2004. The role of the theta isoform of protein kinase C (PKC) in activity-dependent synapse elimination: evidence from the PKC theta knock-out mouse in vivo and in vitro. J. Neurosci. 24, 3762–3769. http://dx.doi.org/10.1523/JNEUROSCI.3930-03.2004 24/15/3762 [pii].

Linda, H., Hammarberg, H., Piehl, F., Khademi, M., Olsson, T., 1999. Expression of MHC class I heavy chain and beta2-microglobulin in rat brainstem motoneurons and nigral dopaminergic neurons. J. Neuroimmunol. 101, 76–86.

Ljunggren, H.G., Van Kaer, L., Sabatine, M.S., Auchincloss Jr., H., Tonegawa, S., Ploegh, H.L., 1995. MHC class I expression and CD8+ T cell development in TAP1/beta 2-microglobulin double mutant mice. Int. Immunol. 7, 975–984.

Looney, M.R., Su, X., Van Ziffle, J.A., Lowell, C.A., Matthay, M.A., 2006. Neutrophils and their Fc gamma receptors are essential in a mouse model of transfusion-related acute lung injury. J. Clin. Invest. 116, 1615–1623. http://dx.doi.org/10.1172/JCI27238.

McConnell, M.J., Huang, Y.H., Datwani, A., Shatz, C.J., 2009. H2-K(b) and H2-D(b) regulate cerebellar long-term depression and limit motor learning. Proc. Natl. Acad. Sci. USA 106, 6784–6789, 0902018106 [pii] 10.1073/pnas.0902018106.

Misgeld, T., Burgess, R.W., Lewis, R.M., Cunningham, J.M., Lichtman, J.W., Sanes, J.R., 2002. Roles of neurotransmitter in synapse formation: development of neuromuscular junctions lacking choline acetyltransferase. Neuron 36, 635–648.

Needleman, L.A., Liu, X.B., El-Sabeawy, F., Jones, E.G., McAllister, A.K., 2010. MHC class I molecules are present both pre- and postsynaptically in the visual cortex during postnatal development and in adulthood. Proc. Natl. Acad. Sci. USA 107, 16999–17004, 1006087107 [pii] 10.1073/pnas.1006087107.

Nelson, P.A., Sage, J.R., Wood, S.C., Davenport, C.M., Anagnostaras, S.G., Boulanger, L. M., 2013. MHC class I immune proteins are critical for hippocampus-dependent memory and gate NMDAR-dependent hippocampal long-term depression. Learn. Mem. 20, 505–517.

Nguyen, Q.T., Lichtman, J.W., 1996. Mechanism of synapse disassembly at the developing neuromuscular junction. Curr. Opin. Neurobiol. 6, 104–112, S0959-4388(96)80015-8 [pii].

Nguyen, Q.T., Parsadanian, A.S., Snider, W.D., Lichtman, J.W., 1998. Hyperinnervation of neuromuscular junctions caused by GDNF overexpression in muscle. Science 279, 1725–1729.

Noutel, J., Hong, Y.K., Leu, B., Kang, E., Chen, C., 2011. Experience-dependent retinogeniculate synapse remodeling is abnormal in MeCP2-deficient mice. Neuron 70, 35–42, S0896-6273(11)00167-X [pii] 10.1016/j.neuron.2011.03.001.

O'Brien, R.A., Ostberg, A.J., Vrbova, G., 1978. Observations on the elimination of polyneuronal innervation in developing mammalian skeletal muscle. J. Physiol. 282, 571–582.

Oliveira, A.L., Thams, S., Lidman, O., Piehl, F., Hokfelt, T., Karre, K., Linda, H., Cullheim, S., 2004. A role for MHC class I molecules in synaptic plasticity and regeneration of neurons after axotomy. Proc. Natl. Acad. Sci. USA 101, 17843–17848.

Pennefather, P., Quastel, D.M., 1981. Relation between subsynaptic receptor blockade and response to quantal transmitter at the mouse neuromuscular junction. J. Gen. Physiol. 78, 313–344.

Perarnau, B., Saron, M.F., Reina San Martin, B., Bervas, N., Ong, H., Soloski, M.J., Smith, A.G., Ure, J.M., Gairin, J.E., Lemonnier, F.A., 1999. Single H2Kb, H2Db and double H2KbDb knockout mice: peripheral CD8+ T cell repertoire and anti-lymphocytic choriomeningitis virus cytolytic responses. Eur. J. Immunol. 29, 1243–1252. http://dx.doi.org/10.1002/(SICI)1521-4141(199904)29:04<1243::AID-IMMU1243>3.0.CO;2-A.

Personius, K.E., Balice-Gordon, R.J., 2001. Loss of correlated motor neuron activity during synaptic competition at developing neuromuscular synapses. Neuron 31, 395–408, S0896-6273(01)00369-5 [pii].

Personius, K., Chang, Q., Bittman, K., Panzer, J., Balice-Gordon, R., 2001. Gap junctional communication among motor and other neurons shapes patterns of neural activity and synaptic connectivity during development. Cell Commun. Adhes. 8, 329–333.

Personius, K.E., Chang, Q., Mentis, G.Z., O'Donovan, M.J., Balice-Gordon, R.J., 2007. Reduced gap junctional coupling leads to uncorrelated motor neuron firing and precocious neuromuscular synapse elimination. Proc. Natl. Acad. Sci. USA 104, 11808–11813.

Personius, K.E., Karnes, J.L., Parker, S.D., 2008. NMDA receptor blockade maintains correlated motor neuron firing and delays synapse competition at developing neuromuscular junctions. J. Neurosci. 28, 8983–8992, 28/36/8983 [pii] 10.1523/JNEUROSCI.5226-07.2008.

Pfeiffer, B.E., Zang, T., Wilkerson, J.R., Taniguchi, M., Maksimova, M.A., Smith, L.N., Cowan, C.W., Huber, K.M., 2010. Fragile X mental retardation protein is required for synapse elimination by the activity-dependent transcription factor MEF2. Neuron 66, 191–197, S0896-6273(10)00188-1 [pii] 10.1016/j.neuron.2010.03.017.

Rafuse, V.F., Polo-Parada, L., Landmesser, L.T., 2000. Structural and functional alterations of neuromuscular junctions in NCAM-deficient mice. J. Neurosci. 20, 6529–6539, 20/17/6529 [pii].

Rall, G.F., Mucke, L., Oldstone, M.B., 1995. Consequences of cytotoxic T lymphocyte interaction with major histocompatibility complex class I-expressing neurons in vivo. J. Exp. Med. 182, 1201–1212.

Redfern, P.A., 1970. Neuromuscular transmission in new-born rats. J Physiol 209, 701–709.

Rees, D., 1978. A non-phosphate-buffered physiological saline for in vitro electrophysiological studies on the mammalian neuromuscular junction [proceedings]. J Physiol 278, 8P–9P.

Roche, S.L., Sherman, D.L., Dissanayake, K., Soucy, G., Desmazieres, A., Lamont, D.J., Peles, E., Julien, J.P., Wishart, T.M., Ribchester, R.R., et al., 2014. Loss of glial neurofascin155 delays developmental synapse elimination at the neuromuscular junction. J. Neurosci. 34, 12904–12918. http://dx.doi.org/10.1523/JNEUROSCI.1725-14.2014.

Rolleke, U., Flugge, G., Plehm, S., Schlumbohm, C., Armstrong, V.W., Dressel, R., Uchanska-Ziegler, B., Ziegler, A., Fuchs, E., Czeh, B., et al., 2006. Differential expression of major histocompatibility complex class I molecules in the brain of a New World monkey, the common marmoset (*Callithrix jacchus*). J. Neuroimmunol. 176, 39–50. http://dx.doi.org/10.1016/j.jneuroim.2006.04.015.

Rudolf, R., Khan, M.M., Labeit, S., Deschenes, M.R., 2014. Degeneration of neuromuscular junction in age and dystrophy. Front. Aging Neurosci. 6, 99. http://dx.doi.org/10.3389/fnagi.2014.00099.

Samuel, N.M., Mirsky, R., Grange, J.M., Jessen, K.R., 1987. Expression of major histocompatibility complex class I and class II antigens in human Schwann cell cultures and effects of infection with *Mycobacterium leprae*. Clin. Exp. Immunol. 68, 500–509.

Sanes, J.R., Lichtman, J.W., 1999. Development of the vertebrate neuromuscular junction. Annu. Rev. Neurosci. 22, 389–442. http://dx.doi.org/10.1146/annurev.neuro.22.1.389.

Sleigh, J.N., Grice, S.J., Burgess, R.W., Talbot, K., Cader, M.Z., 2014. Neuromuscular junction maturation defects precede impaired lower motor neuron connectivity in Charcot-Marie-Tooth type 2D mice. Hum. Mol. Genet. 23, 2639–2650. http://dx.doi.org/10.1093/hmg/ddt659.

Please cite this article in press as: Tetruashvily, M.M., et al. MHCI promotes developmental synapse elimination and aging-related synapse loss at the vertebrate neuromuscular junction. Brain Behav. Immun. (2016), http://dx.doi.org/10.1016/j.bbi.2016.01.008

Smith, L.K., He, Y., Park, J.S., Bieri, G., Snethlage, C.E., Lin, K., Gontier, G., Wabl, R., Plambeck, K.E., Udeochu, J., et al., 2015. Beta2-microglobulin is a systemic pro-aging factor that impairs cognitive function and neurogenesis. Nat. Med. 21, 932–937. http://dx.doi.org/10.1038/nm.3898.

Smits, K.M., Kuppen, P.J., Eggermont, A.M., Tamatani, T., Miyasaka, M., Fleuren, G.J., 1994. Rat interleukin-2-activated natural killer (A-NK) cell-mediated lysis is determined by the presence of CD18 on A-NK cells and the absence of major histocompatibility complex class I on target cells. Eur. J. Immunol. 24, 171–175.

Stevens, B., Allen, N.J., Vazquez, L.E., Howell, G.R., Christopherson, K.S., Nouri, N., Micheva, K.D., Mehalow, A.K., Huberman, A.D., Stafford, B., et al., 2007. The classical complement cascade mediates CNS synapse elimination. Cell 131, 1164–1178.

Strait, R.T., Hicks, W., Barasa, N., Mahler, A., Khodoun, M., Kohl, J., Stringer, K., Witte, D., Van Rooijen, N., Susskind, B.M., et al., 2011. MHC class I-specific antibody binding to nonhematopoietic cells drives complement activation to induce transfusion-related acute lung injury in mice. J. Exp. Med. 208, 2525–2544. http://dx.doi.org/10.1084/jem.20110159.

Syken, J., Grandpre, T., Kanold, P.O., Shatz, C.J., 2006. PirB restricts ocular-dominance plasticity in visual cortex. Science 313, 1795–1800.

Tang, G., Gudsnuk, K., Kuo, S.H., Cotrina, M.L., Rosoklija, G., Sosunov, A., Sonders, M. S., Kanter, E., Castagna, C., Yamamoto, A., et al., 2014. Loss of mTOR-dependent macroautophagy causes autistic-like synaptic pruning deficits. Neuron 83, 1131–1143. http://dx.doi.org/10.1016/j.neuron.2014.07.040.

Tapia, J.C., Wylie, J.D., Kasthuri, N., Hayworth, K.J., Schalek, R., Berger, D.R., Guatimosim, C., Seung, H.S., Lichtman, J.W., 2012. Pervasive synaptic branch removal in the mammalian neuromuscular system at birth. Neuron 74, 816–829, S0896-6273(12)00385-6 [pii] 10.1016/j.neuron.2012.04.017.

Tetruashvily, M.A., Melson, J.W., Park, J.J., Peng, X., Boulanger, L.M., Expression and alternative splicing of classical and nonclassical MHCI genes in the hippocampus and neuromuscular junction. Mol. Cell. Neurosci. in press.

Thams, S., Brodin, P., Plantman, S., Saxelin, R., Karre, K., Cullheim, S., 2009. Classical major histocompatibility complex class I molecules in motoneurons: new actors at the neuromuscular junction. J. Neurosci. 29, 13503–13515, 29/43/13503 [pii] 10.1523/JNEUROSCI.0981-09.2009.

Thompson, W., 1983. Synapse elimination in neonatal rat muscle is sensitive to pattern of muscle use. Nature 302, 614–616.

Thompson, W.J., 1985. Activity and synapse elimination at the neuromuscular junction. Cell. Mol. Neurobiol. 5, 167–182.

Thompson, W., Kuffler, D.P., Jansen, J.K., 1979. The effect of prolonged, reversible block of nerve impulses on the elimination of polyneuronal innervation of newborn rat skeletal muscle fibers. Neuroscience 4, 271–281.

Tsai, N.P., Wilkerson, J.R., Guo, W., Maksimova, M.A., DeMartino, G.N., Cowan, C.W., Huber, K.M., 2012. Multiple autism-linked genes mediate synapse elimination via proteasomal degradation of a synaptic scaffold PSD-95. Cell 151, 1581–1594, S0092-8674(12)01425-0 [pii] 10.1016/j.cell.2012.11.040.

Valdez, G., Tapia, J.C., Kang, H., Clemenson Jr., G.D., Gage, F.H., Lichtman, J.W., Sanes, J.R., 2010. Attenuation of age-related changes in mouse neuromuscular synapses by caloric restriction and exercise. Proc. Natl. Acad. Sci. USA 107, 14863–14868, 1002220107 [pii] 10.1073/pnas.1002220107.

Valdez, G., Tapia, J.C., Lichtman, J.W., Fox, M.A., Sanes, J.R., 2012. Shared resistance to aging and ALS in neuromuscular junctions of specific muscles. PLoS One 7, e34640. http://dx.doi.org/10.1371/journal.pone.0034640 PONE-D-12-03398 [pii].

Vugmeyster, Y., Glas, R., Perarnau, B., Lemonnier, F.A., Eisen, H., Ploegh, H., 1998. Major histocompatibility complex (MHC) class I $KbDb^{-/-}$ deficient mice possess functional CD8+ T cells and natural killer cells. Proc. Natl. Acad. Sci. USA 95, 12492–12497.

Wareham, A.C., Morton, R.H., Meakin, G.H., 1994. Low quantal content of the endplate potential reduces safety factor for neuromuscular transmission in the diaphragm of the newborn rat. Br. J. Anaesth. 72, 205–209.

Wood, S.J., Slater, C.R., 2001. Safety factor at the neuromuscular junction. Prog. Neurobiol. 64, 393–429, S0301008200000551 [pii].

Xu, K., Jha, S., Hoch, W., Dryer, S.E., 2006. Delayed synapsing muscles are more severely affected in an experimental model of MuSK-induced myasthenia gravis. Neuroscience 143, 655–659. http://dx.doi.org/10.1016/j.neuroscience.2006.09.022.

Yamamoto, Y., Henderson, C.E., 1999. Patterns of programmed cell death in populations of developing spinal motoneurons in chicken, mouse, and rat. Dev. Biol. 214, 60–71. http://dx.doi.org/10.1006/dbio.1999.9413.

Zijlstra, M., Li, E., Sajjadi, F., Subramani, S., Jaenisch, R., 1989. Germ-line transmission of a disrupted beta 2-microglobulin gene produced by homologous recombination in embryonic stem cells. Nature 342, 435–438.

Please cite this article in press as: Tetruashvily, M.M., et al. MHCI promotes developmental synapse elimination and aging-related synapse loss at the vertebrate neuromuscular junction. Brain Behav. Immun. (2016), http://dx.doi.org/10.1016/j.bbi.2016.01.008